SUPPLEMENTARY INFORMATION

VORTEX REPRESENTATION

The Josephson junction array described by Eq. (1) can alternatively be viewed in a dual vortex picture. Performing a Villain transformation [34, 35], one obtains the vortex Hamiltonian

$$H = \frac{\pi E_J}{2} \sum_{ij} (m_i - f) G(\mathbf{r}_i - \mathbf{r}_j)(m_j - f), \tag{S1}$$

where i and j run over the N^2 lattice sites located at $\mathbf{r}_i$ and

$$G(\mathbf{r}) = \frac{\pi}{N^2} \sum_{\mathbf{k}\neq 0} \frac{e^{i\mathbf{k}\cdot\mathbf{r}} - 1}{2 - \cos(k_x x) - \cos(k_y y)}. \tag{S2}$$

The components of $\mathbf{k}$ are quantized in multiples of $\frac{2\pi}{N}$. We use the vortex representation for the calculations underlying Fig. 2.

For a given combination of elementary building blocks of striped vortex lattices, e.g., aac, we compute the energy via Eq. (S1) for $\nu = 1/2$. We then increase the magnetic field in units of $1/N^2$ by adding vortices to the channels. We minimize the energy of a given lattice structure by means of a metropolis algorithm. We also use this algorithm to decide to which channel the additional vortex is added. Finally, we allow the partially filled diagonals to shift against each other, which significantly decreases the energies of the c and d structures. We use system sizes $N \sim 100$, chosen in such a way that they are commensurate with the structure (i.e., for c structures, we choose system sizes which are a multiple of 14, for aac, N is chosen as a multiple of 26, etc.) We find that the energies do not exhibit significant N dependence if N is increased further.

We comment on trends evident in Fig. 2(f) of the main text. In the region $\frac{1}{3} < f < \frac{5}{14}$ (red), the building blocks of type a have a natural frustration $f = \frac{1}{3}$, while the channels c are stable for frustrations larger than $f = \frac{5}{14}$ corresponding to half-filled channels. This implies that alternations of a and c are stable beyond minimal frustrations, which grow with the fraction of c building blocks. The energy of a particular structure grows rapidly with f, since both the building blocks of type a become energetically less favorable (they are the natural building blocks at $f = \frac{1}{3}$) and the channels c become filled beyond half filling, which adds domain walls. We note that Fig. 2(a) contains only short-period structures. Other, longer-period structures are likely ground states in some region of frustrations f, although they are not included in the figure.

It is, at least in principle, possible that in some restricted regions of f, the true ground state is not of this striped form, but has a more complicated 2d structure. For instance, partially filled diagonals which are less than half filled destabilize the walls of the channels (see Fig. S1 for corresponding numerical results). It is conceivable that this may destabilize the stripe-like pattern into a more complicated 2d configuration just before the onset of one of the structures.

In the region $\frac{5}{14} < f < \frac{8}{21}$ (blue), the lowest energy structure consists of channels c only, with the partially filled diagonal filling up from being half filled ($f = \frac{5}{14}$) to being two-third filled ($f = \frac{8}{21}$). Thus, one expects that the energy

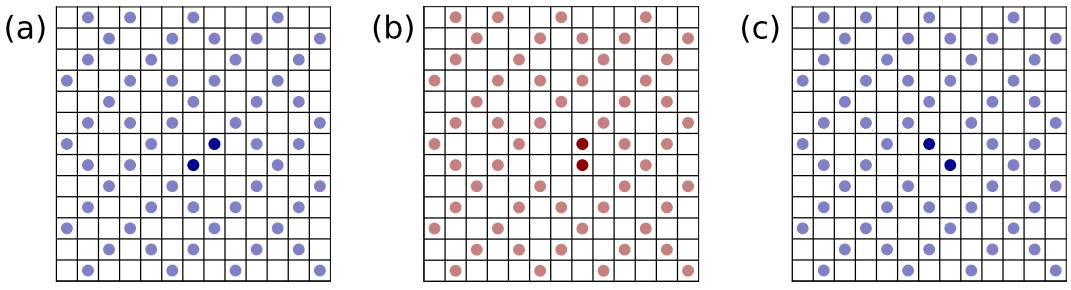

Figure S1. Instability of channels for occupations $\nu < 1/2$ of the partially filled diagonal. (a) Metastable structure with light domain wall. Light domain walls necessarily exist for $\nu < 1/2$. (b) Adjacent saddle-point configuration with a vortex displaced out of a neighboring fully occupied diagonal. (c) Lower-energy minimum reached from the saddle point, in which two vortices have moved out of full diagonal.

of the state increases as f grows within this regime, as indeed observed. Note that beyond $f = \frac{8}{21}$, the partially filled diagonals necessarily contain instances of three consecutive occupied sites. This induces a noticable cusp in the energy of the c configuration vs. frustration.

In the region $\frac{8}{21} < f < \frac{2}{5}$ (green), we find structures that combine channels c with the basic unit b of the $f = \frac{2}{5}$ ground state. As f increases within this region, one thus expects that the b blocks become energetically more favorable, while the c blocks become energetically more costly as the partially filled diagonal increase in occupancy. This is consistent with the weaker f dependence of the configurations combining b and c blocks.

We also note that the bc structure can be competitive with a pure c structure near $f = \frac{8}{21}$, since the filling of the channel is much lower in bc than in c at these frustrations. Similarly, the bcc structure can have a higher energy than the bc structure, since the channels have a larger occupation in bcc than in bc. Eventually, this trend would have to reverse however, as structures of the form bc...c should become close in energy to a pure c configuration, as the number of c building blocks increases.

In the purple region, one expects a transition from channels c to thick channels of type d interspersing b-type building blocks. This transition will presumably happen in the limit of rare interspersing (thick) channels, so that it is masked in Fig. 2, which is limited to short periods.

In the region $\frac{9}{22} < f < \frac{14}{33}$ (orange; not previously identified), we find that the ground state is built from thick channels d, with the partially filled diagonal again varying from half to two-third filling. Compared to the channels c, we observe that the energy of the structure is more weakly dependent on the frustration f.

Finally, we remark that in the white region in Fig. 2(f) beyond $f = \frac{14}{33}$, it is conceivable that the ground states are constructed from $f = \frac{3}{7}$ building blocks, interspersed with thick channels d. Corresponding energies are shown in Fig. S2. We note that the $f = \frac{4}{9}$ stripe structure is no longer a stable ground state, but preempted by vacancy crystals on top of the $f = \frac{1}{2}$ state. This will eventually preclude additional regimes of stripe structures.

PHASE CONFIGURATIONS

To search for minima and saddle points of the phase configurations, we start from Eq. (1). We can search for the ground-state configuration using the algorithm proposed in Ref. [16]. The algorithm relies on describing the junctions within the RCSJ model and solving the set of Kirchhoff's rules at each lattice site of the array. This results in N^2 coupled linear differential equations. Temperature is incorporated by Langevin currents due to Johnson-Nyquist noise. Starting from a random initial configuration of the phases, one computes the time evolution of the system while temperature is gradually decreased to zero. We use periodic boundary conditions, which requires N to be a multiple of q for a frustration of $f = p/q$.

In the range $f = 1/3$ to $f = 1/2$, a direct application of this algorithm [16] tends to result in configurations with domain walls. We avoid this by applying a slightly larger magnetic field along diagonals, where the expected vortex lattice has nonzero vortex occupation (and compensate on empty diagonals to leave the overall magnetic flux fixed). Following the annealing process, we revert to a uniform magnetic field and adjust the phase configuration using a steepest-decent algorithm. We find no change of the vortex configuration in this process.

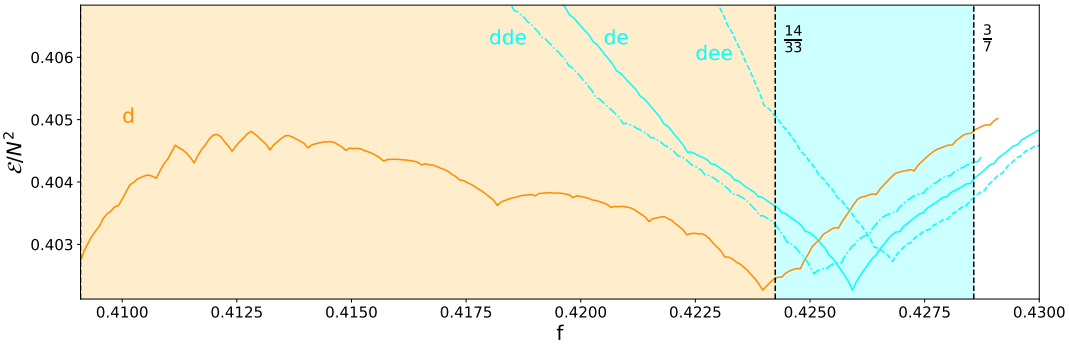

Figure S2. Energy $\mathcal{E}$ per lattice site of various vortex-lattice structures as a function of f. This figure extends Fig. 2(f) beyond $f = 14/33$ up to $f = 3/7$. In this region, the ground states likely consist of combinations of thick channels (building block d) and building block e (three filled diagonals alternating with four empty diagonals, corresponding to the elementary unit of the $f = \frac{3}{7}$ structure).

We use the following parameters in our simulations: Josephson coupling $E_J = 1$, normal resistance $R = 1$, $n = 10^5$ time steps, step size $\Delta\tau = 0.5$, initial temperature $T_0 = 0.2$. For the first 2×10^4 time steps, temperature is held constant after which it is decreased linearly to zero. For the stripe phases, we enhance the frustration on the expected fully occupied diagonals by $\Delta f = 0.1$ and decrease the frustration on one neighboring diagonal by the same amount.

To identify the relevant hopping processes of vortices, we proceed as follows. We apply the climbing-string method described in the next section to the phase model in Eq. (1) to identify the adjacent saddle point. Subsequently, we follow the steepest descent to find the final-state minima. We also confirm the resulting activiation barriers using the vortex model. Note, however, that the vortex model describes a discrete set of vortex configurations. Thus, it cannot describe the entire activation path, but only initial, final, and saddle configurations.

CLIMBING-STRING METHOD

We compute the energy barrier between two minima of the vortex lattice using the climbing-string method, see Ref. [32]. The idea behind this saddle-point search is to start with a phase configuration close to a minimum and to reverse the force pushing the phases into the minimum. This converges to an adjacent saddle point in a controlled manner. We briefly summarize the essential steps and detail the numerical values of parameters used in the simulations.

Step 1: We denote the minimum of the vortex lattice by the vector $\mathbf{\Phi}_0 = (\phi_1, \phi_2, ..., \phi_{N^2})$. We start with an initial random configuration $\mathbf{\Phi}_M$ close to $\mathbf{\Phi}_0$. We linearly interpolate between these two configurations to obtain $M-1$ images $\mathbf{\Phi}_i$ with $i = 1, ..., M-1$, which form a string with the end points $\mathbf{\Phi}_0$ and $\mathbf{\Phi}_M$. We now keep $\mathbf{\Phi}_0$ fixed and evolve the images according to the equations of motion

$$\dot{\mathbf{\Phi}}_i = -\boldsymbol{\nabla} H, \quad 0 < i < M \tag{S3}$$

$$\dot{\mathbf{\Phi}}_M = -\boldsymbol{\nabla} H + \theta(\boldsymbol{\nabla} H \cdot \boldsymbol{\tau})\boldsymbol{\tau}. \tag{S4}$$

with $\theta > 1$ and the approximate tangent vector $\boldsymbol{\tau}$ given by

$$\boldsymbol{\tau} = \frac{\mathbf{\Phi}_M - \mathbf{\Phi}_{M-1}}{|\mathbf{\Phi}_M - \mathbf{\Phi}_{M-1}|}. \tag{S5}$$

The endpoint $\mathbf{\Phi}_M$ is thus climbing up the basin of the minimum $\mathbf{\Phi}_0$ in the tangent direction of the string, while following steepest decent dynamics in the perpendicular direction. The other points of the string are moving towards the minimum.

Step 2: To ensure that the endpoint converges to an adjacent saddle point, one checks after k timesteps whether the energy rises monotonically along the string. If there is an image $\mathbf{\Phi}_J$ with $H(\mathbf{\Phi}_J) > H(\mathbf{\Phi}_{J+1})$, the string is truncated at $\mathbf{\Phi}_J$. Furthermore, the set of images is rebalanced such that they remain evenly distributed along the string. We parametrize the images in terms of the arclength, computed as

$$s_0 = 0, \quad s_{i+1} = s_i + |\mathbf{\Phi}_{i+1} - \mathbf{\Phi}_i|. \tag{S6}$$

The parameters of the images are then given by

$$\alpha_i^* = s_i / s_J. \tag{S7}$$

The images with their associated parameters are used to calculate an analytic expression for the string via, e.g., cubic interpolation. The curve $\gamma = \{\mathbf{\Phi}(\alpha), \quad \alpha \in [0,1]\}$ is evaluated at $\alpha = i/M$ for $0 \leq i \leq M$ to recover a set of evenly distributed images.

Step 3: We check whether the endpoint of the string converged to a saddle point by the condition

$$\max\{|\boldsymbol{\nabla} H(\mathbf{\Phi}_M)|, \quad 0 \leq i \leq N^2\} < \delta \tag{S8}$$

with a tolerance δ. If not, one repeats the previous steps until convergence.

For a striped vortex lattice configuration $\mathbf{\Phi_0} = (\phi_{11}, \phi_{12}, ...)$ with a domain wall at site (ij), we use the initial configuration $\mathbf{\Phi_M} = (\phi'_{11}, \phi'_{12}, ...)$ with

$$\phi'_{i+1,j+1} = \phi_{i+1,j+1} + 2. \tag{S9}$$

and otherwise identical phases. This choice ensures that the saddle point is connected to a domain-wall hop. We further use $M = 20$ images, a time step $\Delta t = 0.01$, a force parameter $\theta = 1.2$, and a tolerance $\delta = 0.0001$. We rebalance the images after $k = 500$ time steps. The bond energy E_J is set to unity.